Journal of Catalysis 280 (2011) 247–254

Contents lists available at ScienceDirect

Journal of Catalysis

journal homepage: www.elsevier.com/locate/jcat

Layered niobic acid with self-exfoliatable nanosheets and adjustable acidity for catalytic hydration of ethylene oxide

Zhi-Jian Yang [a], Ye-Fei Li [b], Qing-Bin Wu [a], Nan Ren [a], Ya-Hong Zhang [a], Zhi-Pan Liu [b,*], Yi Tang [a,*]

[a] Department of Chemistry, Shanghai Key Laboratory of Molecular Catalysis Innovative Materials and Laboratory of Advanced Materials, Fudan University, Shanghai 200433, PR China
[b] Key Laboratory for Computational Physical Sciences, Ministry of Education, Shanghai Key Laboratory of Molecular Catalysis and Innovative Materials, Department of Chemistry, Fudan University, Shanghai 200433, PR China

ARTICLE INFO

Article history:
Received 4 February 2011
Revised 24 March 2011
Accepted 25 March 2011
Available online 6 May 2011

Keywords:
Ethylene oxide
Catalytic hydration
Monoethylene glycol
Layered niobic acid
Self-exfoliation

ABSTRACT

Layered niobic acids ($H_xK_{1-x}Nb_3O_8$, $x = 0–1$) are reported as new solid acid catalysts for the selective hydration of ethylene oxide (EO). They are prepared by simply calcinating Nb_2O_5–K_2CO_3 mixture followed by an ion-exchange process in HNO_3 solution of different concentrations. The highest selectivity for monoethylene glycol (MEG) is achieved over 95% with EO conversion of >99% at x of 0.7 under H_2O/EO ratio of 8. Combined with the results of first-principles density functional theory calculations and Hammett indicator method, it is revealed that the suitable acid strength is more crucial for MEG selectivity than acid amount. Furthermore, a self-exfoliation of layered HNb_3O_8 is also found during EO hydration, which proves to be another important factor for its good catalytic performance by exposing the abundant acid sites among the $Nb_3O_8^-$ nanosheets. The thermal stability investigation of HNb_3O_8 also indicates a careful selection of characterization and application way for this layered niobic acid.

1. Introduction

As an adaptable intermediate, monoethylene glycol (MEG) has found its increasing importance, particularly in the fabrication of polyester fiber. Up to now, catalytic hydration of ethylene oxide (EO) is still a predominant MEG preparation approach. However, a large excess of water (normally H_2O/EO > 20) has to be adopted to compress the production of by-products, causing enormous energy consumption during the distillation process. To improve the MEG selectivity at a relative low H_2O/EO ratio, considerable efforts have been made to explore efficient catalysts such as anion-exchange resins [1–3], supported metal oxides and zeolites [4,5], soluble inorganic salts [6], quaternary phosphoniumhalides [7], polymeric organosilane ammonium salts [8]. However, some apparent drawbacks still exist during the application of these catalysts, such as the swelling of resin, the separation of the catalysts from homogeneous system, and the complexity/high cost for the synthesis of some new catalysts.

Cation-exchangeable layered transition metal oxides are one of the attractive solid acid catalysts due to their enriched ion-exchangeable sites within the interlayer space. The layered metal oxide of $HNbMoO_6{\cdot}nH_2O$ and $HTaMoO_6$ were reported as favorable acid catalysts for various reactions [9–11]. As an important type of solid catalyst, niobic acid (*e.g.*, $Nb_2O_5{\cdot}nH_2O$) has attracted much attention in dehydration, hydration, esterification, hydrolysis, condensation, and alkylation reactions [4,12–17] for its unique acidity in presence of water. Recently, a lot of efforts are continuously focused on the catalytic application of layered niobic acids because of their nanosheet crystal structure and facile preparation via simply ion exchange of protons from their corresponding potassium niobates [18,19]. However, these solid catalysts are usually proved ineffective because the small d-spacing between their two-dimensional (2D) anionic nanosheets with high charge density prevents the penetration of the reactants into the interlayer region. Although the preparation of exfoliated sheets of layered niobic acids via soft-solution pre-exfoliation can overcome the above barrier [15,20–22], it still seems difficult in practical application because of the adoption of expensive agent (*e.g.*, tetrabutylammonium hydroxide, TBAOH) during the redundant exfoliation process. In our present study, layered HNb_3O_8 is found to be capable of *in situ* self-exfoliation in some aqueous catalytic systems, and it is also reasonable to expect a remarkable catalytic activity of this material compared with pre-exfoliated samples.

On the basis of this discovery, herein, we report the first example of the layered $H_xK_{1-x}Nb_3O_8$ as the solid acid catalyst for EO hydration. The exchange degree value (x) can be precisely adjusted by carefully controlling ion-exchange conditions. The acidities of $H_xK_{1-x}Nb_3O_8$ catalysts are systematically characterized by theoretical calculation and Hammett indicator method. It is revealed that a moderate acid strength and the *in situ* self-exfoliation of $H_xK_{1-x}Nb_3O_8$ sheets are crucial for high MEG selectivity besides

* Corresponding authors. Fax: +86 21 65641740.
E-mail addresses: zpliu@fudan.edu.cn (Z.-P. Liu), yitang@fudan.edu.cn (Y. Tang).

0021-9517/$ - see front matter Crown Copyright © 2011 Published by Elsevier Inc. All rights reserved.
doi:10.1016/j.jcat.2011.03.026

the acid amount, and the highest MEG selectivity is achieved over 95% with EO conversion of >99% at x of 0.7. This result is consistent with that in our previous report for the soluble salts/acids catalysts [6], which demonstrated that the best MEG selectivity is achieved within the mild pH range of 3.0–6.0. The conclusions drawn in this work not only considerably inspire the exploitation of new catalyst for EO hydration but are also beneficial for the further understanding of acidic nature, exfoliation effect, and catalytic properties of layered niobic acid. More importantly, the validity of the theoretical calculation on the prediction of acid strength can be proved as well.

2. Experimental

2.1. Preparation of niobic acid catalyst

The chemicals used in the present work including Nb_2O_5, K_2CO_3, HNO_3, ethylene oxide, TBAOH (25%), and deionized water were commercially purchased and used without further purification.

KNb_3O_8 was prepared by molten salt method from a finely grinded mixture of Nb_2O_5 and K_2CO_3 with a slightly excessive amount (10%) of K_2CO_3 to the stoichiometric ratio. The calcination was held at 900 °C for 1 h and then at 1100 °C for 5 h. The KNb_3O_8 product obtained was then washed with hot water to remove the residual K_2CO_3. The phase purity was confirmed by X-ray diffraction (XRD). KNb_3O_8 was then used as the precursor to prepare $H_xK_{1-x}Nb_3O_8$ by a proton-exchange method [23,24]. KNb_3O_8 sample was stirred in a series of HNO_3 solutions with different concentrations (0.2, 2.2, 3.8, 6.5, 10, 20, and 40 wt%) at solution/solid weight ratio of 60 for 48 h to produce $H_xK_{1-x}Nb_3O_8$ with x of 0.11, 0.31, 0.35, 0.49, 0.71, 0.76, and 0.89, respectively. The x values were measured by inductively coupled plasma atomic absorption spectrometry (ICP-AAS). Besides, a fully proton-exchanged sample (HNb_3O_8) was prepared by treating KNb_3O_8 repeatedly in 40 wt% HNO_3 solutions for three times (72 h for each run) at ambient temperature.

The comparative pre-exfoliated HNb_3O_8 was also conducted in TBAOH aqueous solution as reported in previous work [20]. The other two niobic acids of $HNbO_3$ and $H_4Nb_6O_{17}$ were prepared by the similar molten salt synthesis method but with different amount of K_2CO_3 [25,26], followed by repeated acid-exchange treatments.

2.2. Characterization

Scanning electron microscopy (SEM) measurements were performed by a Philips XL30 D6716 instrument at an operating voltage of 25 kV, while transmission electron microscopy (TEM) experiments with selected area electron diffraction (SAED) were carried out with a JEOL JEM-2010 instrument at an operating voltage of 200 kV. XRD patterns were recorded on a Rigaku D/Max-rB 12 kW diffractometer (Cu Kα). N_2 sorption isotherms were recorded with a Micromeritics ASAP 2010 instrument at 77 K. The potassium content in the acid-exchange solution was determined by ICP-AAS (Zeeman-5000). Fourier-transform infrared (FT-IR) spectra were collected on a Nicolet Fourier Spectrophotometer-360 using KBr pellets. Thermogravimetric analysis (TGA) was carried out using a Mettler Toledo TGA-SDTA851 analyzer from 25 to 900 °C under nitrogen with ramp of 5 °C/min.

2.3. Acid strength H_0 determination by Hammett indicator method

The Hammett indicators used were neutral red, methyl red, 4-dimethylamino-azobenzene, crystal violet, and anthraquinone with the pK_a values of +6.8, +4.8, +3.3, +0.8, and −5.6, respectively. The indicators were resolved in dried petroleum ether of reagent grade and its concentration was 0.1 wt% [27]. After drying in vacuum, 100 mg of grinded sample was rapidly transferred into a transparent tube and 2 ml of petroleum ether was injected to cover the sample. Subsequently, several drops of indicator solution were added followed by vigorous shaking. The range of H_0 value was determined by color variation.

2.4. Methodology and theoretical calculation details for acid strength (pK_a)

The acid strength value pK_a of $H_xK_{1-x}Nb_3O_8$ was calculated using the SIESTA package [28] with numerical atomic orbital basis sets [29] and Troullier–Martins norm-conserving pseudopotentials [30]. The exchange–correlation function utilized was GGA-PBE, and the double-ζ plus polarization (DZP) basis set was employed. The semicore 4s and 4p states of Nb were included. The cutoff for the real space grid was set as 150 Ry. The quasi-Newton BFGS method was employed for geometry relaxation until the maximal forces on each relaxed atom were less than 0.1 eV/Å. The solvation energy due to the long-range electrostatic interaction was computed by a periodic continuum solvation model with a smooth dielectric function. The detailed algorithm of the continuum solvation method has been addressed by Fattebert and Gygi [31], which has been implemented by us for the calculations of solvation energies of free molecules and for periodic system previously [32,33]. A large vacuum region (30 Å) along Z-axis that separates two adjacent sheets was introduced. In solving the Poisson–Boltzmann equation numerically, we utilized a sixth-order FD scheme that is appropriate to discretize partial differential equations with periodic boundary conditions [34]. This scheme utilizes the finite-difference stencil to get the symmetric sparse linear system. In terms of the symmetry, the linear system is solved iteratively by a parallel version of MINRES with the preconditioner. To realize a fully parallelism, we chose the incomplete LU preconditioners based on the second-order FD scheme in a localized preconditioner implementation.

The pK_a of the solid acid was calculated by:

$$pK_a = \frac{\Delta G_{diss}}{2.303 k_B T} - 1.74 = 16.88 \Delta G_{diss} - 1.74 \quad (1)$$

where −1.74 is the pK_a of H_3O^+, and ΔG_{diss} is the Gibbs free energy of dissociation:

$$AH + H_2O \rightarrow A^- + H_3O^+ \quad (2)$$

$$\begin{aligned} \Delta G_{diss} &= G(A^-) - G(AH) + G(H_3O^+) - G(H_2O) \\ &= E(A^- - AH) + ZPE(A^- - AH) + G(H_3O^+ - H_2O) \\ &= E(A^- - AH) - 0.27eV - 11.53eV \\ &= E(A^- - AH) - 11.80eV \end{aligned} \quad (3)$$

where −11.53 eV is the free energy difference value between H_3O^+ and H_2O [35].

2.5. Catalytic testing

The hydration reaction of EO was carried out in an isothermal batch autoclave reactor with a typical H_2O/EO molar ratio of 8 under continuous stirring (200 rpm) at 110 °C, and the pressure was kept as 1.5 MPa by N_2. The catalyst amount is normally 3 mmol/mol EO. After a 0.5-h reaction, the reactor was cooled down and the products were analyzed on a GC920 gas chromatograph equipped with a HP-INNOWAX column and a flame ionization detector. Since EO conversion with any catalyst was nearly 100%, MEG selectivity was chiefly taken into account as the criterion

for the comparison of catalyst performance. All the catalysts were easily separated and reused after filtration and drying.

3. Results and discussion

3.1. Structure of layered HNb_3O_8 and catalytic activity for EO hydration

Fig. 1a and b show the SEM images of as-prepared KNb_3O_8 and HNb_3O_8 (after ion exchange in 40 wt% HNO_3 for three times) samples. Both of them show the typical morphology of layered materials with a size of ~20 μm. Fig. 1c shows the XRD patterns of HNb_3O_8 and original Nb_2O_5, and the appearance of characteristic diffraction peaks 020, 120 and 240 of HNb_3O_8 sample indicates its perfect phase purity as reported previously [23,36–37]. The hydration results catalyzed by HNb_3O_8 and some reference catalysts are shown in Table 1. The HNb_3O_8 presents an excellent MEG selectivity of 95%, even close to the best result of homogeneous catalyst (HCOONa) reported recently [6]. Fig. 1d shows the effect of H_2O/EO ratio on MEG selectivity using HNb_3O_8 and HCOONa as catalysts compared with the blank test. Obviously, MEG selectivity in thermal hydration (blank) is always much lower than those in the other two catalyzed systems at every H_2O/EO ratio. It is worth noticing that only 3 mmol of HNb_3O_8 is sufficient to catalyze each mol of EO in this reaction, which is near 100 times lower than that in homogeneous catalytic system (200 mmol/mol EO). Contrarily, the other two niobic acids ($HNbO_3$ and $H_4Nb_6O_{17}$) as well as the cubic Nb_2O_5 exhibit the MEG selectivity almost as poor as thermal hydration in blank test. Such results will be discussed in the following section.

3.2. Effect of self-exfoliation of layered niobic acid

As described in Section 3.1, only HNb_3O_8 shows high MEG selectivity among the three niobic acid catalysts. Fig. 2 shows the SEM and TEM images of these niobic acids after EO hydration reaction. It is obvious that the HNb_3O_8 sample shows a completely different result compared with the other two samples. The thin nanosheets of HNb_3O_8 can be easily observed from its SEM image after reaction, while other two niobic acids remain almost the same morphologies as those before reaction. The existence of ultrathin HNb_3O_8 sheet is further confirmed by TEM experiment on the catalyst freshly collected after reaction (Fig. 2d), and the accompanying SAED pattern clearly shows the sharp diffraction spots (inset of Fig. 2d). Such results obviously indicate that the HNb_3O_8 sample is able to self-exfoliate into crystalline nanosheets in the EO hydration system. In addition, the BET surface area of the layered HNb_3O_8 before reaction is only 2 m^2/g, while it reached to 79 m^2/g after reaction, close to that of the nanosheets exfoliated using TBAOH as reported elsewhere [20]. In the current catalytic system, the self-exfoliated HNb_3O_8 nanosheets would expose a large quantity of acid sites to the reactants, resulting in its excellent catalytic behavior. The poor catalytic capability of $HNbO_3$ and $H_4Nb_6O_{17}$ could be attributed to the absence of this crucial *in situ* self-exfoliation behavior.

Table 1
Initial catalytic performance of HNb_3O_8 and reference samples for EO hydration.

Catalyst	Amount (mmol/mol EO)	MEG selectivity (%)
Blank	–	79.5
Nb_2O_5	3	81.1
HNb_3O_8	3	95.1
HCOONa	200	96.4
$HNbO_3$	3	80.4
$H_4Nb_6O_{17}$	3	79.8

Reaction conditions: at 120 °C, H_2O:EO = 10 mol/mol.

The crystal structure property of the self-exfoliated HNb_3O_8 after EO hydration was further studied by XRD analysis (Fig. 3a, I). It is observed that the self-exfoliated HNb_3O_8 freshly separated

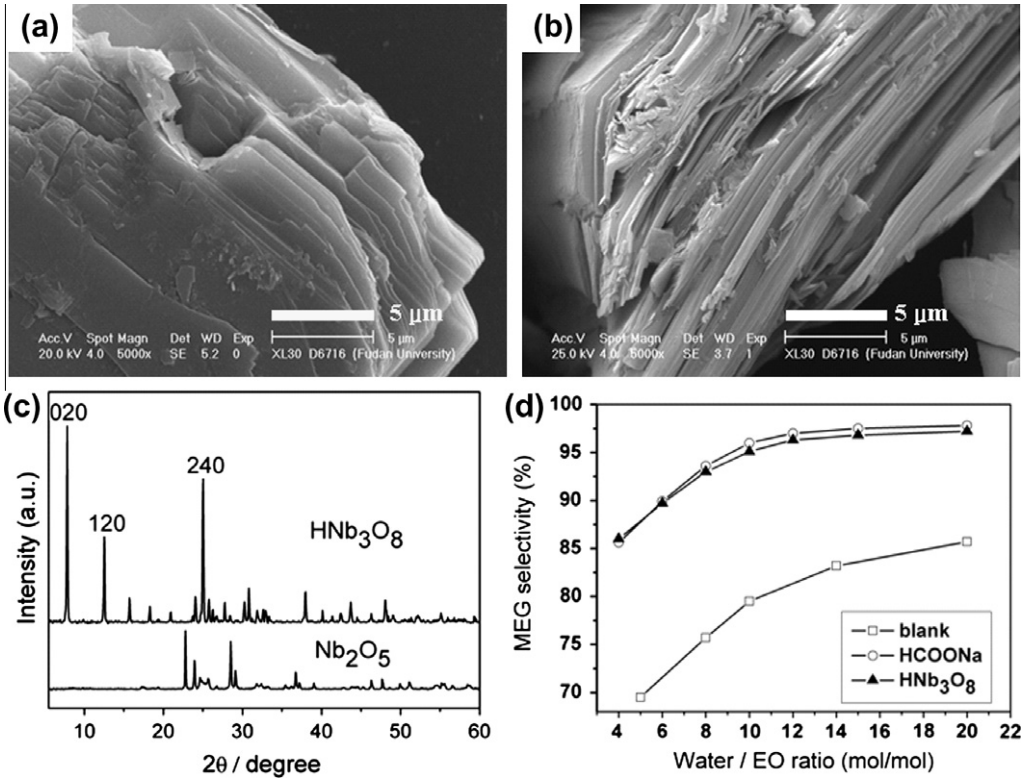

Fig. 1. SEM images of KNb_3O_8 (a) and HNb_3O_8 (b); XRD patterns for HNb_3O_8 and Nb_2O_5 (c); and effect of H_2O/EO ratio on MEG selectivity in HNb_3O_8, HCOONa catalyzed and thermal hydration (blank test).

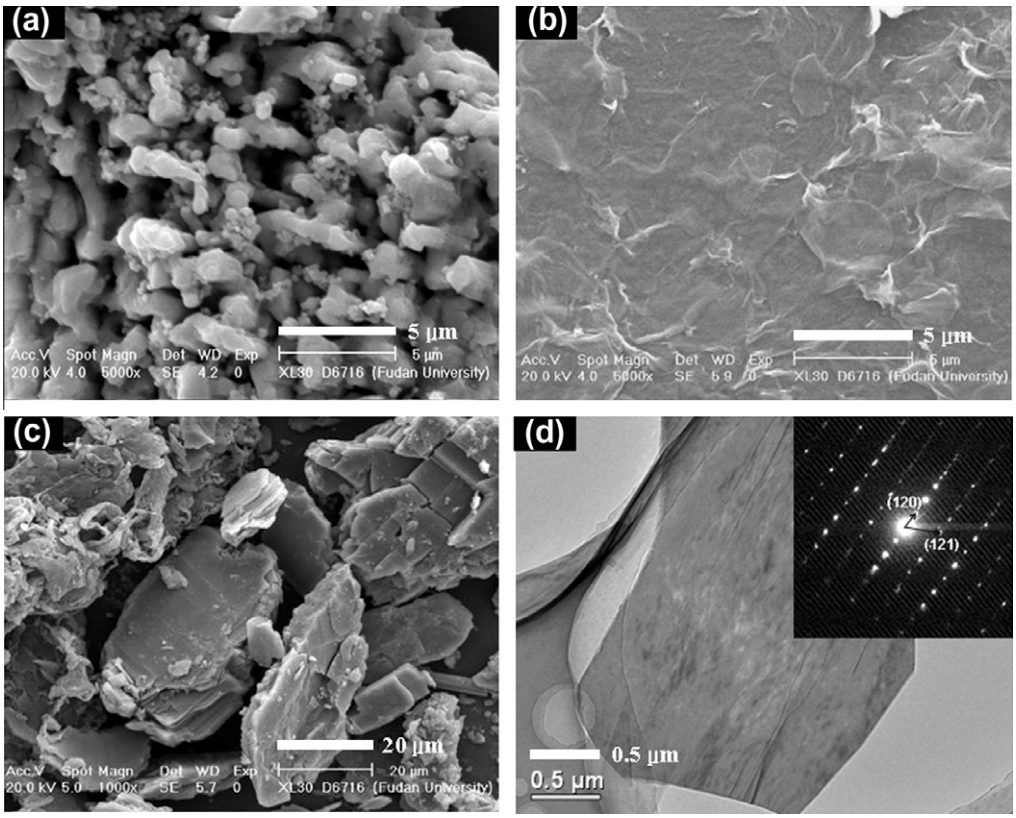

Fig. 2. SEM images of $HNbO_3$ (a), HNb_3O_8 (b), and $H_4Nb_6O_{17}$ (c), and TEM of HNb_3O_8 (d) after reaction. The inset of (d) is the SAED of (d).

from the reaction system (0 h) shows a near amorphous phase, while that after standing for 24 h would recover to its original crystal phase although the peaks are somewhat broadened. This fact further proves that the HNb_3O_8 can self-exfoliate into colloidal nanosheets in reaction system, which can gradually re-stack into its original crystal structure with drying, probably due to the high charge density of the 2D sheets. To confirm the positive effect of self-exfoliation, the layered niobic acid was also pre-exfoliated by TBAOH and evaluated in EO hydration for comparison. Fig. 3b shows the SEM image of HNb_3O_8 after TBAOH pre-exfoliation, in which the exfoliated nanosheets can be clearly observed as those of HNb_3O_8 after reaction (Fig. 2b). XRD patterns of the pre-exfoliated HNb_3O_8 by TBAOH show a similar re-stacking phenomenon compared with the self-exfoliated sample, as shown in Fig. 3a. More interestingly, such pre-exfoliated sample behaves the similar MEG selectivity to the directly used HNb_3O_8, indicating that the pre-exfoliation of HNb_3O_8 is unnecessary for EO hydration. The reusability of the HNb_3O_8 catalyst is further confirmed by putting the re-stacked sample into the reaction system repeatedly, and no obvious change is observed in either activity or MEG selectivity for at least five cycles (Table 2).

To study the mechanism of self-exfoliation, H_2O, EO, MEG, and diethylene glycol (DEG) were used as a single reactant, and all the other reaction conditions were kept constant as before. It is found that no single reactant or product can result in the layer self-exfoliation. Fig. 4 shows the FT-IR characterization results of HNb_3O_8 before and after reaction, and an adsorption peak centered at 3353 cm^{-1} is found in the spectrum of original HNb_3O_8, corresponding to the stretching vibration of O—H bond. The wavenumber shifts to a low value compared to normal O—H stretching probably because of the association effect in the niobic acid layers. In addition, the intensity of O—H stretching vibration peak around

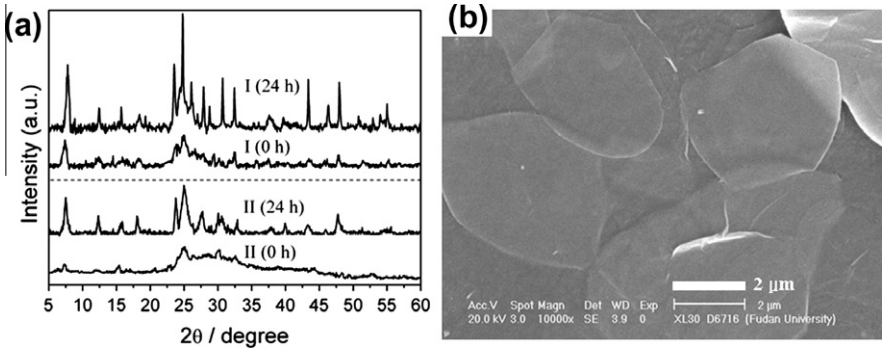

Fig. 3. XRD patterns of the HNb_3O_8 collected freshly after EO hydration reaction (a-I, 0 h) and stood for 24 h (a-I, 24 h), and that collected just after TBAOH exfoliation (a-II, 0 h) and stood for 24 h (a-II, 24 h), and SEM image of TBAOH-exfoliated HNb_3O_8 (b).

Table 2
The recycling performance of HNb_3O_8 in EO catalytic hydration.

Recycle	EO conversion (%)	MEG selectivity (%)
1	99.8	92.2
2	99.6	91.9
3	99.6	91.3
4	98.9	91.6
5	99.1	90.9

Reaction conditions: 110 °C, H_2O:EO = 8 mol/mol, catalyst amount of 3 mmol/mol EO.

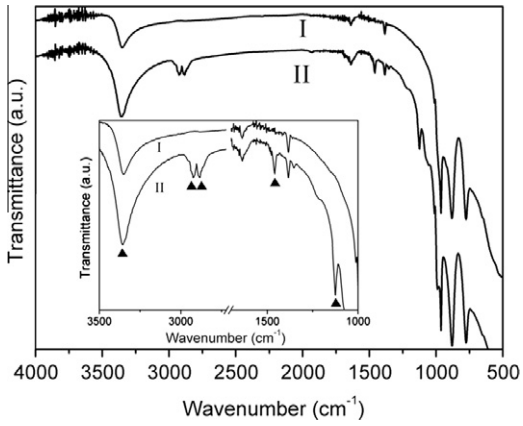

Fig. 4. FT-IR results of original HNb_3O_8 before (I) and after reaction (II). The inset is the enlarged view.

3353 cm^{-1} becomes stronger for the HNb_3O_8 sample after reaction, indicating an extra increase in the amount of hydroxyl, such as alcohol species. The appearance of the peaks at 2933, 2872, and 1462 cm^{-1} could be attributed to the stretching and bending vibration of C—H in methylene, and the peak around 1126 cm^{-1} belongs to the C—O stretching vibration. Since all the samples have been carefully washed for four times and treated with vacuum drying prior to characterization, the appearance of all these new peaks is a powerful proof of the intermediates encapsulation in the interlayer spaces of the HNb_3O_8 sample after reaction. Therefore, the self-exfoliation process must be caused by the interaction of niobic acid sheets and active intermediates formed during this reaction, such as the protonated EO.

3.3. Acidity adjustability of $H_xK_{1-x}Nb_3O_8$ and the effects on reaction

The pervious study indicates that the mild acidity or basicity of homogeneous catalysts is necessary for the high MEG selectivity in EO hydration [6,38]. In order to investigate the adjustability of catalyst acidity and its effect on EO hydration, herein, the niobic acids with a series of ion-exchange degrees, $H_xK_{1-x}Nb_3O_8$ (x = 0–1), were prepared by deliberately adjusting the exchange conditions. Fig. 5 shows the catalytic behavior of the samples with different x values. The EO conversion slightly increases with the increasing of x, and all the samples have the conversion over 90%. Contrarily, MEG selectivity increases rapidly in low x range and decreases at high x values. The best selectivity is obtained at the x value of about 0.5–0.8. Additionally, a mechanical mixture with equimolar amounts of KNb_3O_8 and HNb_3O_8 is used as the counterpart for the niobic acid with the exchange degree of 0.5 ($H_{0.5}K_{0.5}Nb_3O_8$). It is found that the MEG selectivity of $H_{0.5}K_{0.5}Nb_3O_8$ obtained by acidification is much higher than that of the mechanical mixed counterparts (indicated as star point in Fig. 5) in spite of the same proton content in these two samples, indicating the existence of some synergy effects besides acid amount.

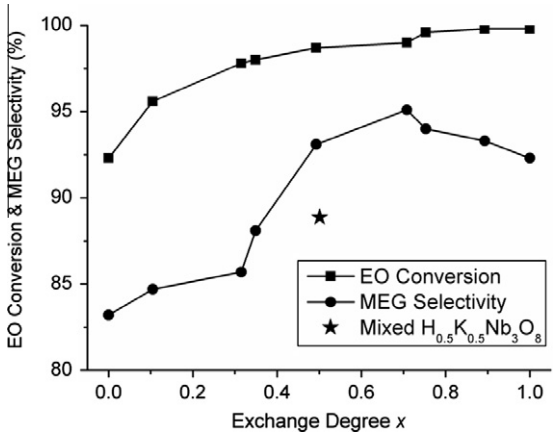

Fig. 5. Effect of x in $H_xK_{1-x}Nb_3O_8$ on MEG selectivity and EO conversion at 110 °C, catalyst amount = 3 mmol/mol EO and H_2O/EO molar ratio = 8.

To further explore the effects of catalyst acidity on EO hydration, the relationship between MEG selectivity and the amount of catalyst with different x is shown in Fig. 6. Two conclusions can be drawn from this experiment:

(1) With the increase in the catalyst amount, all catalysts show an initial dramatic increase in MEG selectivity. However, when catalyst amount is above 3 mmol/mol EO, the amount of catalysts with higher exchange degree ($x \geq 0.49$) presents a negligible influence on the MEG selectivity, while the samples with lower exchange degree ($x \leq 0.35$) still show a slow increasing tendency. The catalyst with $x = 0.7$ presents a highest MEG selectivity at every catalyst amount, consistent with the results in Fig. 5.
(2) The discrepancy of the MEG selectivity between the low proton-exchanged catalysts comparing to those with high ion-exchange degrees cannot be compensated by simply increasing the catalyst amount. For example, even the weight of catalyst with low x value was increased (*e.g.*, x = 0.35, 12 mmol/mol EO) to insure the same acid amount as that with high degree but low weight (*e.g.*, x = 0.7, 6 mmol/mol EO), the selectivity of the former is still much lower than the latter, as shown in Fig. 6.

To explain the above phenomena, both the Hammett indicator method and theoretical calculation are introduced to evaluate

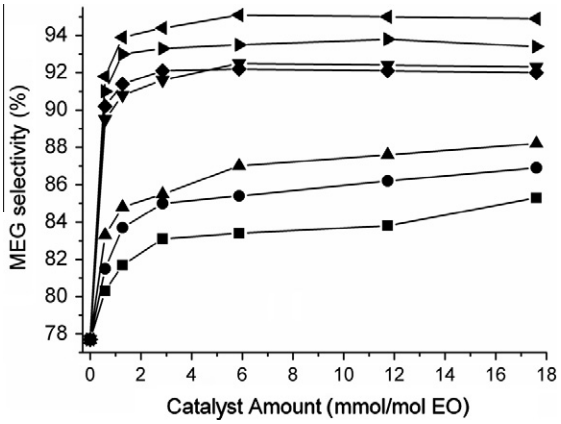

Fig. 6. Effect of catalyst amount on MEG selectivity for series of $H_xK_{1-x}Nb_3O_8$ catalysts under 110 °C and H_2O/EO molar ratio = 8. (-■- x = 0.11, -●- x = 0.31, -▲- x = 0.35, -▼- x = 0.49, - ◄- x = 0.71, -►- x = 0.75, -◆- x = 0.89.)

the acid strength of $H_xK_{1-x}Nb_3O_8$. Table 3 shows the H_0 data of the catalysts with different x measured by series of Hammett indicators with the pK_a values from +6.8 to −5.6. Obviously, the acid strength (H_0) of catalysts increases with the increase of x value. And the acid strength (pK_a) of $H_xK_{1-x}Nb_3O_8$ was further calculated using first-principles density functional theory calculations with a parallel periodic continuum solvation model. The unit cell of layered niobic acid is shown in Fig. 7a, and a rectangular supercell of 15.187 × 18.201 Å is utilized for the surface slab, as in Fig. 7b. Due to the large unit cell, only Γ-point Monkhorst–Pack k-point mesh was routinely utilized for energy and structural calculations. Each sample often possesses the protons with different acid strength due to the differences in chemical micro-environment, and Fig. 8a shows the pK_a of the protons with the strongest acid strength. Obviously, the pK_a value decreases from 14 to −10 with the increase in x, which indicates that, besides their acid amount, the higher exchange degree can also cause stronger acid strength. This tendency is consistent with that of H_0 data measured by Hammett indicator method (Table 3), but the theoretical pK_a values span a larger range compared to the experimental ones. Such discrepancy can be interpreted by the different cases in these two methods:

(1) The measured H_0 in titration experiment probably reflects only the acidity on the external surface because the $H_xK_{1-x}Nb_3O_8$ sample is existed in its un-exfoliated state during the measuring process, and large Hammett indicator molecules cannot intercalate into the interlayer spaces to contact the internal surface. On the contrary, the models in the theoretical calculation are free to simulate the protons in any kinds of micro-environment on the slab.

(2) In the H_0 experiment, it is supposed that the acid sites are homogeneously distributed in both the external and internal surface, and therefore, the H_0 data detected on the external surface can represent the acid strength of all the sites in the sample. However, it seems not the case according to results of the theoretical calculation. This is very likely that K^+ ion generally prefers to expose to the solution (*i.e.*, on the external surface) because of its large electrostatic solvation energy. We have utilized the following Eqs. (4) and (5) to establish the possibility of the inhomogeneous exchange degree at various exchange conditions, which is defined as the energy change (E_1 and E_2) of the reactions.

$$x_{sur} + x_{bulk} \rightarrow (x - 0.125)_{sur} + (x + 0.125)_{bulk} \quad (4)$$

$$x_{sur} + x_{bulk} \rightarrow (x + 0.125)_{sur} + (x - 0.125)_{bulk} \quad (5)$$

$$E_1 = E_{sur} + (x - 0.125) + E_{bulk}(x + 0.125) - E_{sur}(x) - E_{bulk}(x) \quad (6)$$

$$E_2 = E_{sur} + (x + 0.125) + E_{bulk}(x - 0.125) - E_{sur}(x) - E_{bulk}(x) \quad (7)$$

Table 3
Acid strength distribution of $H_xK_{1-x}Nb_3O_8$ with different x values.

Sample	x value	pK_a values of Hammett indicators [a]					Summary	Calculation
		+6.8	+4.8	+3.3	+0.8	−5.6	H_0 [b]	pK_a [c]
$H_{0.11}K_{0.89}Nb_3O_8$	0.11	–	–	–	–	–	>6.8	15
$H_{0.31}K_{0.69}Nb_3O_8$	0.31	+	–	–	–	–	6.8–4.8	8–7
$H_{0.35}K_{0.65}Nb_3O_8$	0.35	+	–	–	–	–	6.8–4.8	7–6
$H_{0.49}K_{0.51}Nb_3O_8$	0.49	+	+	±	–	–	3.3	4
$H_{0.71}K_{0.29}Nb_3O_8$	0.71	+	+	+	–	–	3.3–0.8	−1
$H_{0.75}K_{0.25}Nb_3O_8$	0.75	+	+	+	–	–	3.3–0.8	−3
$H_{0.89}K_{0.11}Nb_3O_8$	0.89	+	+	+	±	–	0.8	−7
HNb_3O_8	1	+	+	+	+	–	0.8 to −5.6	−10

[a] "+" stands for discolored, "–" for not discolored and "±" for transitional color.
[b] Summarized from the discoloration results of Hammett indicators.
[c] Calculated from the theoretical model as shown in Fig. 8a.

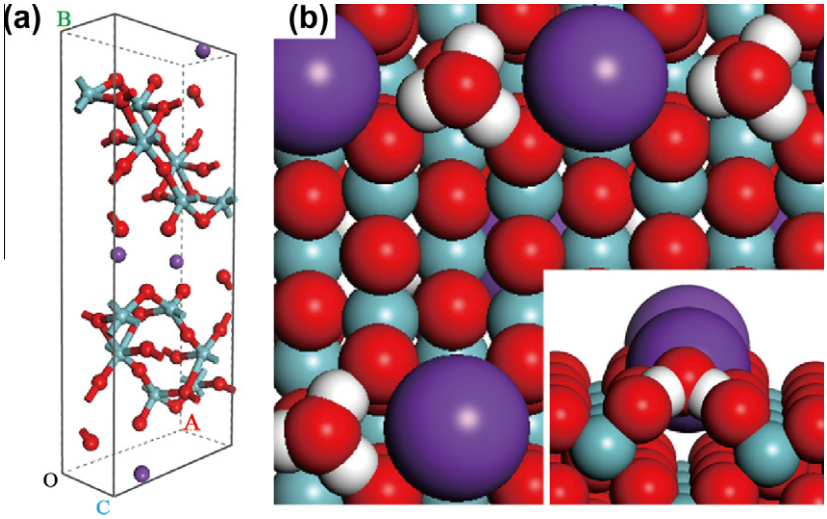

Fig. 7. Unit cell of 3.796 × 9.100 × 21.837 Å (a), side view (b), and top view (insert) of computer model of $H_xK_{1-x}Nb_3O_8$. K, purple; O, red; H, white; Nb, blue. (For interpretation of the references to color in this figure legend, the reader is referred to the web version of this article.)

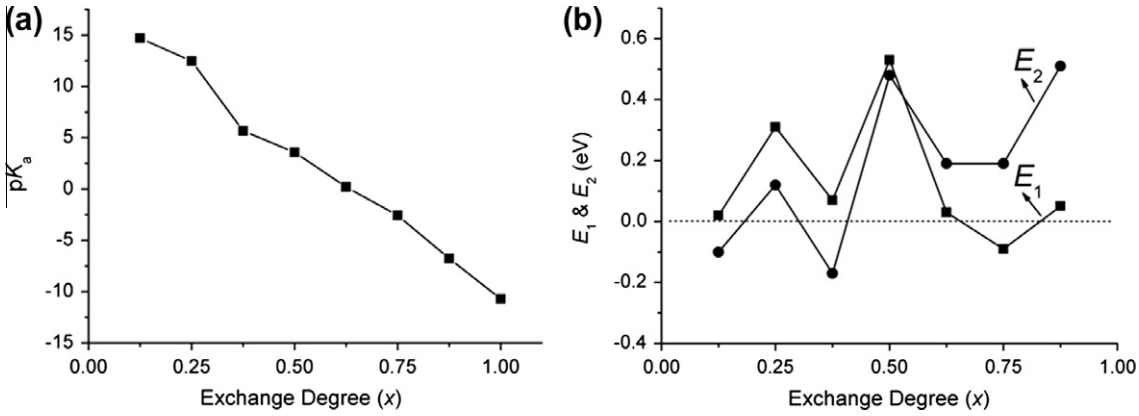

Fig. 8. Calculated pK_a value (a) and E_1 and E_2 (b) of different exchange degrees.

where x is the exchange degree, and 0.125 is the quasi-differential exchange degree from calculations. A negative E_1/E_2 indicates the surface prefers a lower/higher exchange degree than the bulk. It is expected that a stable surface should have positive E_1 and E_2 simultaneously. The calculated E_1 and E_2 are plotted in Fig. 8b. Interestingly, we have found that there are two specific stable exchange degrees (*i.e.*, 0.25 and 0.5) whose E_1 and E_2 are both highly positive. In particular, once the exchange degree exceeds 0.5, E_1 becomes negative or close to zero, indicating the surface prefers to decrease its exchange degree. This proves that the inconsistency in the calculated pK_a and the measured H_0 at the high exchange degree may well be caused by the low exchange degree on surface. Therefore, the theoretical calculation model can provide more suitable method to illustrate the acid strength distribution in such a layer-structured catalyst because it can precisely determine the acid strength both in the external and in the internal surface. The acid sites on the internal surface should be more crucial for the reaction like EO hydration in which the catalyst layers tend to self-exfoliate to expose the internal acid sites.

By combining the acidity data (Table 3 and Fig. 8a) with the reaction results (Figs. 5 and 6), it is found that the acid strength may be the factor more crucial on MEG selectivity than the acid amount. Both the experimental characterization and the theoretical calculation show the monotonous decrease of the H_0 or pK_a (*i.e.*, the increase in the acid strength) with the increase of the x, but the catalyst presents a volcano-like curve with the highest selectivity at the x = ca. 0.7. Therefore, the acid sites with mild strength are the keys for the high MEG selectivity in EO hydration reaction, and too weak or too strong acid strength will lead to the decline of MEG selectivity.

3.4. Thermal stability of niobic acid catalysts

Fig. 9a shows the XRD patterns of pure HNb_3O_8 after calculating at different temperatures for 6 h in air. The XRD patterns are changed into those of R-Nb_2O_5 [39] when the heating temperature is above 210 °C. The catalytic tests show that HNb_3O_8 treated below 180 °C exhibits the same catalytic capability as the parent sample, while the samples treated above 210 °C show an absolute inactivation although the layered structure is still maintained from SEM experiment (not shown). Fig. 9b shows the TG/DTA results of pure HNb_3O_8, which is similar to previous report [37,39]. The first step of weight loss below 150 °C is attributed to the dehydration from $HNb_3O_8{\cdot}H_2O$ to HNb_3O_8. The second weight loss step started from 200 °C corresponding to the phase transformation from HNb_3O_8 to R-Nb_2O_5. The TG/DTA results are in good accordance with the XRD patterns and corresponding reaction performance. Therefore, both the acidity characterization (*e.g.*, the Hammett indicator method) and application of this layered HNb_3O_8 as a solid acid catalyst can only be conducted at a relative low temperature. The fact might also imply that some normally used characterization methods relying on adsorption/desorption temperature of alkaline molecules, such as NH_3 temperature programmed desorption or pyridine IR-adsorption, are difficult to precisely determine the acidity of catalysts like layered niobic acids that are thermally unstable.

4. Conclusions

Layered niobic acids ($H_xK_{1-x}Nb_3O_8$, x = 0–1) are proposed as the new solid acid catalysts for EO hydration. The highest selectivity

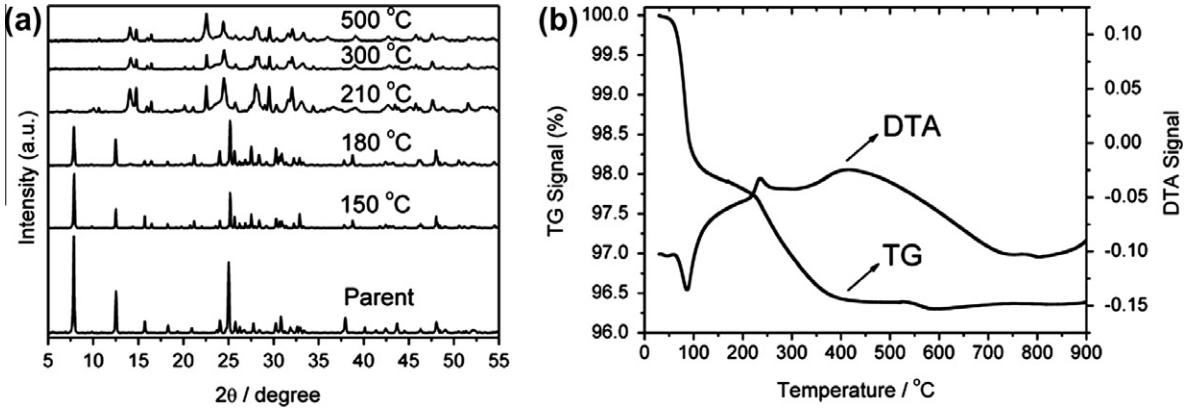

Fig. 9. XRD patterns after being treated at different temperatures (a) and TG/DTA results (b) of pure HNb_3O_8.

for MEG is achieved over 95% with EO conversion of >99% under H_2O/EO ratio of 8 and catalyst/EO of 3 mmol/mol. An *in situ* self-exfoliation behavior of $Nb_3O_8^-$ nanosheets during the EO hydration is found and proved as one of the most crucial factors for its high MEG selectivity. More importantly, the acidity of $H_xK_{1-x}Nb_3O_8$ can be precisely adjusted via simple proton-exchange process, and the catalysts present a volcano-like curve with the highest selectivity at the *x* of ca. 0.7. Combined with the results of theoretical calculation and Hammett indicator method, which show the monotonous increase in acid strength of $H_xK_{1-x}Nb_3O_8$ with the ion-exchange degree, it is concluded that the acid strength is more important for MEG selectivity than acid amount. The low-cost preparation, facile acidity adjustability, and unique self-exfoliation/re-stacking property of layered niobic acids make them the efficient catalysts in the aqueous systems, such like the case in EO hydration reaction of this paper.

Acknowledgments

This work was supported by NSFC (20890122, 21073041, 20825311), the STCSM (075211013, 09JC1401200, 09DZ2271500, 10QH1400300) and the Major State Basic Research Development Program of China (2009CB623506, 2009CB930403), 863 Programme (2009AA033701) and Program for Professor of Special Appointment (Eastern Scholar) at Shanghai Institute of Higher Learning.

References

[1] G.R. Strickler, V.G. Landon, G.J. Lee, W.J. Rievert, US Patent 6 137 015, 2000; US Patent 6 160 187, 2000.
[2] V. Kruchten, W. Derks, US Patent 6 580 008, 2003.
[3] F.P. Yu, H. Cai, W.J. He, W.M. Yang, Z.K. Xie, J. Appl. Polym. Sci. 115 (2010) 2946.
[4] Y.C. Li, S.R. Yan, L.P. Qian, W.M. Yang, Z.K. Xie, Q.L. Chen, B. Yue, H.Y. He, J. Catal. 241 (2006) 173.
[5] T. Maihom, S. Namuangruk, T. Nanok, J. Limtrakul, J. Phys. Chem. C 112 (2008) 12914.
[6] Z.J. Yang, N. Ren, Y.H. Zhang, Y. Tang, Catal. Commun. 11 (2010) 447.
[7] K. Kawabe, US Patent 6 080 897, 2000.
[8] V. Kruchten, US Patent 5 874 653, 1999.
[9] C. Tagusagawa, A. Takagaki, S. Hayashi, K. Domen, J. Am. Chem. Soc. 130 (2008) 7230.
[10] C. Tagusagawa, A. Takagaki, K. Takanabe, K. Ebitani, S. Hayashi, K. Domen, J. Catal. 270 (2010) 206.
[11] A. Takagaki, C. Tagusagawa, K. Domen, Chem. Commun. 42 (2008) 5363.
[12] K. Tanabe, S. Okazaki, Appl. Catal. A: Gen. 133 (1995) 191.
[13] K. Tanabe, W.F. Holderich, Appl. Catal. A: Gen. 181 (1999) 399.
[14] A.S. Dias, S. Lima, D. Carriazo, V. Rives, M. Pillinger, A.A. Valente, J. Catal. 244 (2006) 230.
[15] X.J. Guo, W.H. Hou, W.P. Ding, Y.N. Fan, Q.J. Yan, Y. Chen, Micropor. Mesopor. Mater. 80 (2005) 269.
[16] I. Nowak, M. Ziolek, Chem. Rev. 99 (1999) 3603.
[17] K. Tanabe, Catal. Today 78 (2003) 65.
[18] C. Tagusagawa, A. Takagaki, K. Takanabe, K. Ebitani, S. Hayashi, K. Domen, J. Phys. Chem. C 113 (2009) 17421.
[19] M.A. Bizeto, A.L. Shiguiharab, V. Constantino, J. Mater. Chem. 19 (2009) 2512.
[20] A. Takagaki, D. Lu, J.N. Kondo, M. Hara, S. Hayashi, K. Domen, Chem. Mater. 17 (2005) 2487.
[21] A. Takagaki, M. Sugisawa, D. Lu, J.N. Kondo, M. Hara, K. Domen, S. Hayashi, J. Am. Chem. Soc. 125 (2003) 5479.
[22] A. Takagaki, T. Yoshida, D. Lu, J.N. Kondo, M. Hara, K. Domen, S. Hayashi, J. Phys. Chem. B 108 (2004) 11549.
[23] X.K. Li, N. Kikugawa, J.H. Ye, Adv. Mater. 20 (2008) 3816.
[24] X.K. Li, N. Kikugawa, J.H. Ye, Chem. Eur. J. 15 (2009) 3538.
[25] T. Rojac, M. Kosec, M. Połomska, B. Hilczer, P. Segedin, A. Bencan, J. Eur. Ceram. Soc. 29 (2009) 2999.
[26] G.B. Saupe, C.C. Waraksa, H.N. Kim, Y.J. Han, D.M. Kaschak, D.M. Skinner, T.E. Mallouk, Chem. Mater. 12 (2000) 1556.
[27] K.Y. Wang, X.S. Wang, G. Li, Micropor. Mesopor. Mater. 94 (2006) 325.
[28] J.M. Soler, E. Artacho, J.D. Gale, A. Garcia, J. Junquera, P. Ordejon, D. Sanchez-Portal, J. Phys.: Condens. Matter 14 (2002) 2745.
[29] J. Junquera, O. Paz, D. Sanchez-Portal, E. Artacho, Phys. Rev. B 64 (2001) 235111.
[30] N. Troullier, J.L. Martins, Phys. Rev. B 43 (1991) 1993.
[31] J.L. Fattebert, F. Gygi, Phys. Rev. B 73 (2006) 115124.
[32] H.F. Wang, Z.P. Liu, J. Phys. Chem. C 113 (2009) 17502.
[33] Y.F. Li, Z.P. Liu, L.L. Liu, W.G. Gao, J. Am. Chem. Soc. 132 (2010) 13008.
[34] B. Fornberg, D.M. Sloan, Acta Numer. 3 (1994) 203.
[35] M.D. Tissandier, K.A. Cowen, W.Y. Feng, E. Gundlach, M.H. Cohen, A.D. Earhart, J.V. Coe, T.R. Tuttle, J. Phys. Chem. A 102 (1998) 7787.
[36] J.F. Liu, X.L. Li, Y.D. Li, J. Cryst. Growth 247 (2003) 419.
[37] G. Yang, Y.G. Liu, W.H. Hou, H.M. Ji, Y.H. Li, J. Appl. Polym. Sci. 113 (2009) 78.
[38] J.W. van Hal, J.S. Ledford, X.K. Zhang, Catal. Today 123 (2007) 310.
[39] R. Nedjar, M.M. Borel, B. Raveau, Mater. Res. Bull. 20 (1985) 1291.